MEASUREMENTS OF SPEED OF RESPONSE OF HIGH-SPEED VISIBLE AND IR OPTICAL DETECTORS

by H. Edward Rowe and John S. Osmundson

Goddard Space Flight Center
Greenbelt, Md. 20771

NATIONAL AERONAUTICS AND SPACE ADMINISTRATION • WASHINGTON, D. C. • AUGUST 1972

1. Report No. NASA TN D-6874	2. Government Accession No.	3. Recipient's Catalog No.
4. Title and Subtitle Measurements of Speed of Response of High-Speed Visible and IR Optical Detectors		5. Report Date August 1972
		6. Performing Organization Code
7. Author(s) H. Edward Rowe and John S. Osmundson		8. Performing Organization Report No. G-1074
9. Performing Organization Name and Address Goddard Space Flight Center Greenbelt, Maryland 20771		10. Work Unit No. 11. Contract or Grant No.
12. Sponsoring Agency Name and Address National Aeronautics and Space Administration Washington, D.C. 20546		13. Type of Report and Period Covered Technical Note 14. Sponsoring Agency Code

15. Supplementary Notes

16. Abstract

A technique for measuring speed of response of high-speed visible and IR optical detectors to mode-locked Nd:YAG laser pulses is described. Results of measurements of response times of four detectors are presented. Three detectors that can be used as receivers in a 500-MHz optical communication system are tested.

17. Key Words (Selected by Author(s))	18. Distribution Statement
Optical detectors, Lasers, Mode-locking, Optical pulses, Optical communications	Unclassified—Unlimited

19. Security Classif. (of this report)	20. Security Classif. (of this page)	21. No. of Pages	22. Price*
Unclassified	Unclassified	13	$3.00

*For sale by the National Technical Information Service, Springfield, Virginia 22151.

CONTENTS

MEASUREMENTS OF SPEED OF RESPONSE OF HIGH-SPEED VISIBLE AND IR OPTICAL DETECTORS

H. Edward Rowe and John S. Osmundson*
Goddard Space Flight Center

INTRODUCTION

Mode-locked Nd:YAG lasers are extremely attractive candidates as transmitters for high data-rate optical spacecraft communication systems. Nd:YAG lasers have broad gain curves, typically as wide as 120 GHz at the 1.06-μm lasing transition (Reference 1). For a laser of this type with axial mode spacings on the order of several hundred megahertz, it is experimentally possible to lock more than 100 axial modes in phase with one another when the laser is operating in single TEM_{00} mode by inserting an intracavity perturbation varying in time at a frequency equal to the axial mode spacing (References 2 and 3).

This locking of axial modes is known as mode-locking and converts the continuous wave output of the Nd:YAG laser into a pulsed output with the pulse repetition rate given by $f_m = c/2L$, where f_m is the pulse repetition rate in hertz, c is the speed of light in vacuum, and L is the optical path length of the laser cavity.

The width of a mode-locked pulse is inversely proportional to the number of modes locked in phase. The full width of a loss-modulated mode-locked pulse at half amplitude τ_p can be given in terms of measurable parameters (Reference 4), as

$$\tau_p = \frac{\sqrt{\sqrt{2}\ln 2}}{\pi}\left(\frac{g_0}{\delta}\right)^{1/4}\left(\frac{1}{f_m\,\Delta f}\right)^{1/2}, \tag{1}$$

where g_0 is the saturated midband gain of the laser, δ is the depth of modulation of the mode-locking element, f_m is the mode-locked frequency, and Δf is the width of the laser gain curve in hertz. If $g_0 = 0.1$, $\delta = 0.1$, $f_m = 300$ MHz, and $\Delta f = 120$ GHz, then $\tau_p = 50$ ps.

Thus the output of a mode-locked laser consists of a very fast stream of extremely short pulses that is compatible with a digital communication system. One of the most promising methods of transmitting data with a mode-locked laser is pulse-coded modulation (PCM) (References 5 to 7). In PCM a modulator external to the mode-locked laser can code the optical pulse train. The modulator can block a pulse to signify a 0 and let a pulse pass to signify a 1, in a 1,0 binary code.

*National Research Council Resident Research Associate at GSFC.

The pulse-coded data can be received very simply by direct detection with detectors that have response at 1.06 μm. When the system is operating in a low background condition, the only requirement on the detector is that it respond with sufficient speed to the high-pulse-rate input so that the detector output can be processed without introducing intersymbol interference.

Figure 1 shows a stream of optical pulses incident on an optical detector and the resultant detector output. T is the period between adjacent pulses, τ_r is the detector rise time between the 0- and 100-percent levels of the pulse, and τ_f is the detector fall time between the 100- and 0-percent levels of the pulse. Ignoring noise and pulse jitter, if the output of the detector is sampled once every period T, T must be greater than or equal to τ_r and T must be greater than or equal to τ_f to eliminate intersymbol interference. An improved signal-to-noise condition can be obtained, however, by integrating the detector output over one pulse period; for this case the condition for no intersymbol interference is $T \geqslant \tau_r + \tau_f$.

These constraints on the speed of response of detectors in a PCM optical communication system show the need to be able to accurately measure rise and fall times of high-speed optical detectors. In the sections that follow, some of the theory relevant to testing the speed of response of optical detectors to mode-locked pulse trains will be briefly presented and an experiment to measure the speed of response of detectors to a mode-locked Nd:YAG laser output and the results of tests of four high-speed detectors will be described.

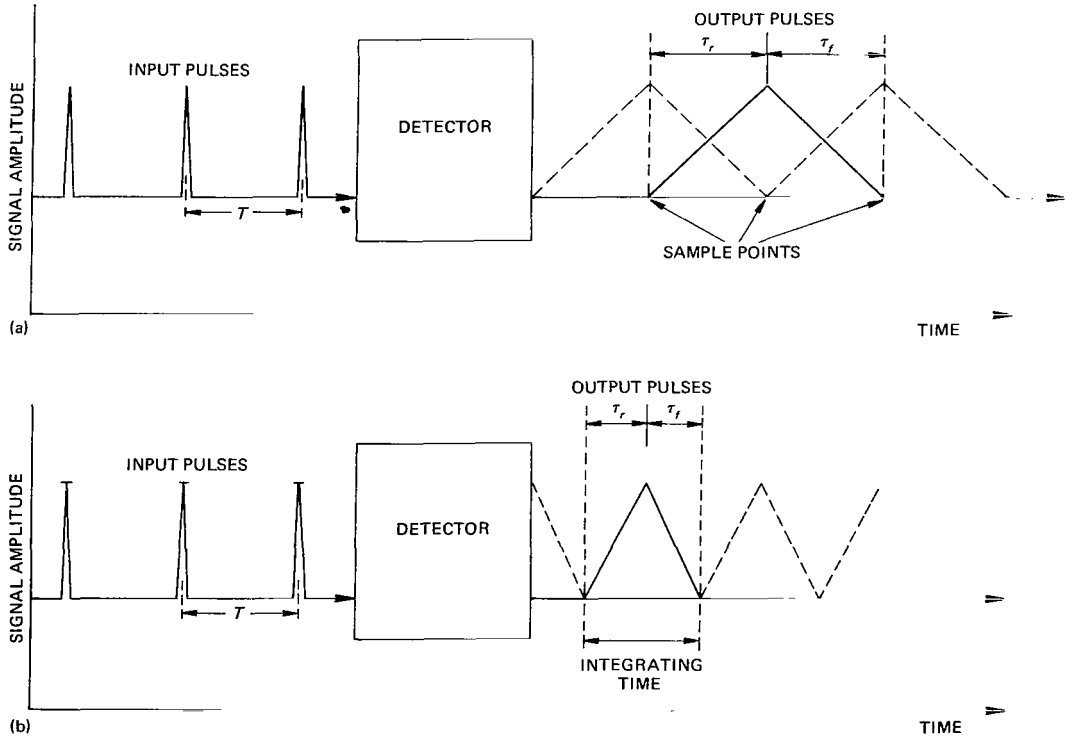

Figure 1—(a) Sampling detection. (b) Integrating detection.

THEORY

The output pulses of a mode-locked laser are gaussian in time and the mode-locked power at the fundamental laser frequency w at any instant in time over one pulse period is given by

$$P_w(t) = P_0 e^{-\alpha t^2} , \tag{2}$$

where α is a constant and P_0 is the peak power of a single mode-locked pulse.

One common measure of pulsewidth is τ_p; using Equation 2

$$\tau_p = 2\sqrt{\frac{\ln 2}{\alpha}} . \tag{3}$$

The 1.06-μm IR output of a Nd:YAG laser can be partially converted into the visible spectrum by frequency doubling the fundamental radiation. This is most easily accomplished by propagating the fundamental radiation through a crystal that absorbs two 1.06-μm photons and reemits one photon at twice the energy, or at a wavelength of 0.53 μm, which is a green wavelength (Reference 8). The second harmonic power in this type of two-photon process is proportional to the square of the incident power, and the instantaneous second harmonic power at $2w$ over one pulse period is given by

$$P_{2w}(t) = KP_w^2(t) = KP_0^2 e^{-2\alpha t^2} , \tag{4}$$

where K is a constant for a given doubling crystal temperature and optical alinement.

Therefore the pulsewidth of the second harmonic pulses is given by

$$\tau_p = \sqrt{\frac{2 \ln 2}{\alpha}} . \tag{5}$$

Thus pulses at the second harmonic are a factor of $\sqrt{2}$ narrower than pulses at the fundamental frequency.

The fundamental pulse exiting from the second harmonic generating crystal is now

$$P_w(t) = P_0 e^{-\alpha t^2}(1 - KP_0 e^{-\alpha t^2}) . \tag{6}$$

This is a nongaussian pulse with a broader pulsewidth than the incident fundamental pulses. In practice, however, the maximum value of K attained during detector testing was $K = 2.5 \times 10^{-5}$ mW^{-1}, and the maximum TEM_{00} laser output during these tests was below 1000 mW. Thus

$$P_w(t) = P_0 e^{-\alpha t^2}(1 - 0.025 e^{-\alpha t^2}) \text{ mW} \tag{7}$$

is the worst possible case of pulse degradation, and for this instance τ_p is changed by no more than 2.5 percent.

In any actual laboratory test of a detector, the output of the detector must be passed through electronic components that have finite frequency response and act as frequency filters. If several pass-band filters of the same bandwidth are cascaded, the overall bandwidth is given by

$$\Delta f_n = \Delta f_1 \sqrt{2^{1/n} - 1}\ , \tag{8}$$

where Δf_n is the bandwidth of a cascade of n filters each with bandwidth Δf_1.

The rise time of such a cascade (Reference 9) will then be given by

$$\tau_r \cong \sqrt{n}\tau_1\ . \tag{9}$$

If the filters do not have identical bandwidths, then the rise time of the cascade (Reference 9) will be given by

$$\tau_r = \sqrt{\tau_1^2 + \tau_2^2 + \cdots + \tau_n^2}\ , \tag{10}$$

where τ_i is the rise time of the ith filter.

The term "rise time" usually refers to response time between the 10- and 90-percent points of the leading edge of a pulse, and fall time usually refers to the response time between the 90- and 10-percent points of the trailing edge of a pulse. This convention will be used in the following sections.

EQUIPMENT

A block diagram of the experiment for testing 1.06-μm detectors is shown in Figure 2a. The laser has a 3- by 50-mm Nd:YAG rod, pumped in a double elliptical cavity by two tungsten lamps, and is operated in the TEM_{00} mode.

A loss modulator driven at approximately 136 MHz by an amplified frequency synthesizer was used as the mode-locking element. This produced a mode-locked pulse train with a repetition rate twice the drive frequency, or approximately 272 MHz.

The mode-locked 1.06-μm laser output was split into two beams by a beamsplitter. One beam of the fundamental output was detected by a photodiode,[1] the output of which was sent into a sampling head and then displayed on one channel of a sampling oscilloscope. The second 1.06-μm beam was detected by the device to be tested; the output of this detector was sent into the second port of the sampling head and displayed simultaneously on the second channel of the sampling oscilloscope.

Detectors with responses in the visible spectrum were tested with the experimental array shown in Figure 2b. The fundamental 1.06-μm mode-locked laser beam was externally focused into a $Ba_2NaNb_5O_{15}$ crystal where it was partially converted into its second harmonic at 0.53 μm. The beam exiting from the barium sodium niobate was collimated and then the 0.53-μm radiation was separated from the fundamental beam by a dichroic beamsplitter. Signals from the two detectors were processed identically as in Figure 2a.

In each test an appropriate 1.06- or 0.53-μm passband filter, 10 nm wide, was placed in front of each detector. This insured that most of the radiation detected was the mode-locked laser output.

[1] In this case a Coherent Optics model 32 photodiode.

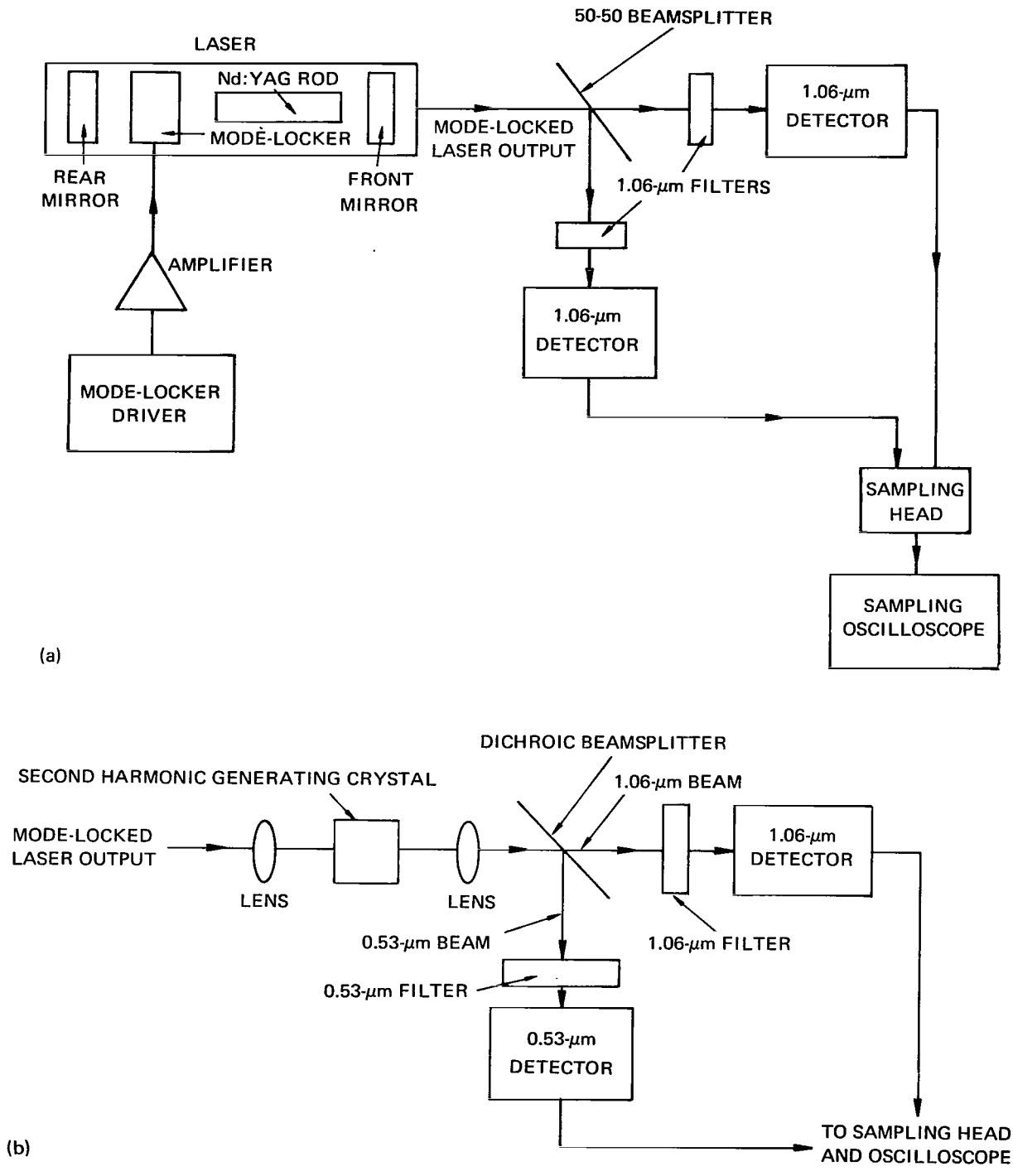

Figure 2—Experimental array for measuring response times of detectors. (a) 1.06-μm detector measurement. (b) 0.53-μm detector measurement.

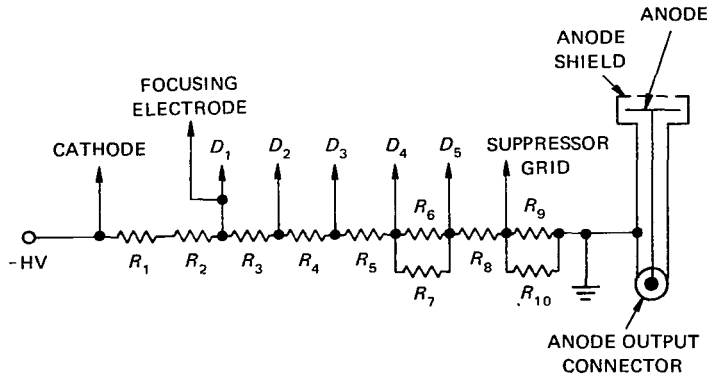

Figure 3—Voltage divider of the second detector. R_1 to R_7: 510 kΩ, 1 W; R_8: 470 kΩ, 1 W; R_9 and R_{10}: 82 kΩ, 1 W.

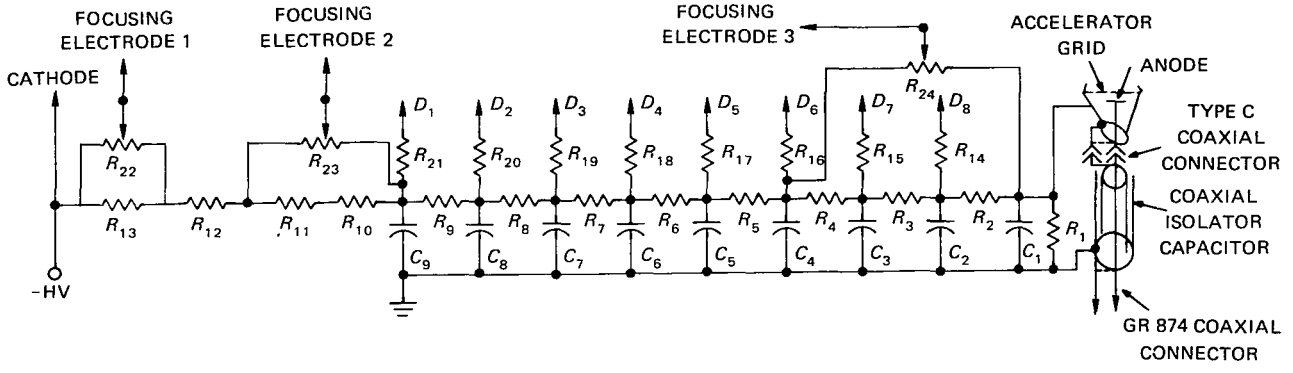

Figure 4—Voltage divider chain of the third detector. R_1, R_{14} to R_{21}: 100 kΩ, ½ W; R_2 to R_{10}, R_{12}, R_{13}: 200 kΩ, 1 W; R_{11}: 300 kΩ, 1 W; R_{22}: 5 MΩ; R_{23} and R_{24}: 10 MΩ; c_1: 0.1 μf; c_2 to c_9: 0.01 μf.

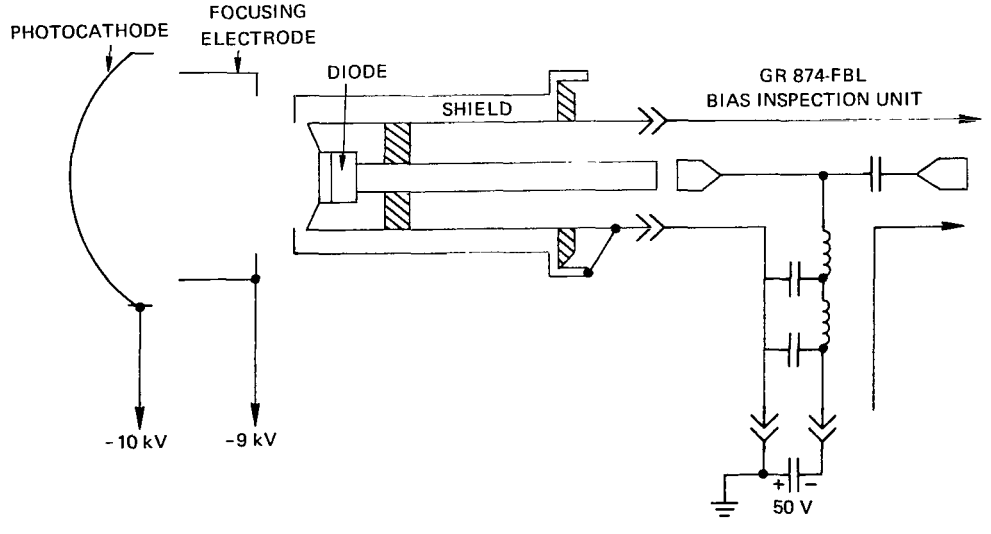

Figure 5—Silicon multiplier and voltage bias network.

Four high-speed detectors were tested. The first of these, a crossed-field photomultiplier,[2] was designed for applications requiring high time resolution, and its frequency response is specified by the manufacturer to be from dc to 3 GHz. Therefore, it should have a rise time of about 100 ps. It has an S1 photocathode that has response to both visible and near-IR radiation, and the tube has a nominal gain of 2×10^4. The multiplier contains nine dynodes and utilizes both static electric and crossed magnetic fields. The tube is terminated into a slotted 50-Ω coaxial transmission line, and connection to an external 50-Ω load is provided.

The second detector tested was a photomultiplier designed for applications requiring subnanosecond time response.[3] It has electrostatic focusing and in-line dynodes and provides a gain of 5×10^6. Its rise time is specified to be less than 1 ns at an operating voltage of 3500 V. The anode is terminated with a coaxial pin sealed in the tube envelope and is supplied with a 15-cm coaxial adaptor assembly with a mating connector on one end and a GR 874 connector on the other. The voltage divider used was selected for best response time and is shown in Figure 3.

A special-purpose high-speed photomultiplier[4] was the third device tested. It has eight dynodes and an S20 photocathode. Its gain is 10^5 at 5000 V and its rise time is specified to be less than 1 ns. The multiplier has a focused linear construction and delivers pulses into a 50-Ω coaxial line sealed in the tube base; the line is terminated in a standard C-type connector. Figure 4 shows a schematic of the voltage divider chain.

The fourth detector tested was a silicon multiplier.[5] This is an experimental device consisting of a photocathode, a focusing electrode, and a photodiode. The input light is incident on the photocathode, and photoelectrons emitted by the photocathode are then focused onto the photodiode. In principle this will give the time response of a photodiode and also have gain of about 10^3. The response of the unit tested has not been optimized because the components of the device were chosen because of availability rather than for optimal characteristics. The manufacturer feels that with the proper selection of components the response can be improved, especially the fall time. Figure 5 shows a schematic of the silicon multiplier and voltage bias network.

RESULTS

Figures 6a and 6b are photographs of single sweeps on the sampling oscilloscope of tests of the first detector, the crossed-field photomultiplier. The upper trace in each photograph shows the response of the photodiode to the incoming 1.06-μm mode-locked pulse train and the lower trace is the response of the crossed-field photomultiplier to the same input. (Sweeps just above or through detector response traces on some pictures are the response of the same detector when the input is blocked.) The time scale for both traces is 1 ns/cm. Figure 6b is identical to Figure 6a except that the time scale on Figure 6b is 500 ps/cm.

Equation 10 may be rewritten as

$$\tau_x = \sqrt{\tau^2_{\text{output}} - \tau^2_{\text{signal}} - \tau^2_{\text{sampler}}},$$

[2]Sylvania model 502. [3]RCA C 31024. [4]ITT F 4102. [5]ITT SSX037101.

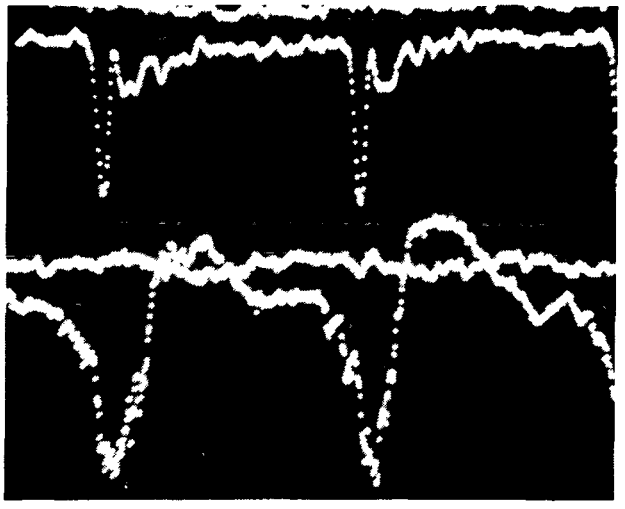

(a)

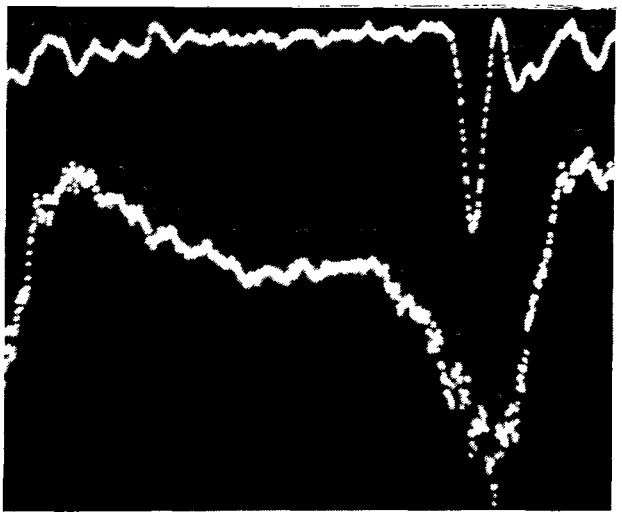

(b)

Figure 6—The upper trace on both parts of the figure shows the photodiode response to 1.06-μm pulses (vertical scales: 5 mV/cm). The lower trace on both parts of the figure is the crossed-field photomultiplier (the first detector) response to the same 1.06-μm pulses (vertical scales: 2 mV/cm). (a) Time scale: 1 ns/cm. (b) Time scale: 500 ps/cm.

where τ_x is the rise time of the detector being studied, τ_{output} is the rise time of the signal as observed on the lower trace of Figure 6a or b, and $\tau_{sampler}$ is the rise time of the sampling oscilloscope. The signal rise time τ_{signal} can be measured by setting

$$\tau_{signal} = \sqrt{\tau^2_{output} - \tau^2_{diode} - \tau^2_{sampler}}$$

and using the upper trace of Figure 6a or b to give the output rise time. The sampler response is given as 90 ps. The diode rise time is given as $\tau_{diode} < 100$ ps, and here is assumed to be equal to 80 ps.[6]

From direct measurement of Figure 6a, it is found that $\tau_r = 670$ ps for the first detector. A similar analysis can be used on the fall time, giving $\tau_f = 550$ ps. A linear leading and trailing edge on the pulses is assumed so that these rise and fall times, multiplied by 1.2, will be equal to the full rise and fall times shown on Figure 1. With this assumption the crossed-field photomultiplier has adequate response to detect mode-locked pulses 200 ps wide at a 670-MHz repetition rate without introducing intersymbol interference.

Response of the tube was measured as a function of tube operating voltage; results shown in Figures 6a and b were for a tube voltage of 3800 V, the optimum operating voltage. The crossed-field photomultiplier shows overshoot at the end of each pulse; this may be due to a space charge near the anode at the end of each pulse. Also, the time response of this detector is close to an order of magnitude worse than the manufacturer's specifications.

Oscillations are always seen on the trailing edge of the photodiode response curve. This type of ringing is a common occurrence with fast diodes and is usually due in main part to an impedance mismatch between the photodiode and the 50-Ω line connecting it to the sampling head.

[6]Diode rise time is estimated in the following way: For $g_0 = 0.02$, $\delta = 0.18$ rad (for an FM mode-locker), $\Delta f = 120$ GHz, and $f_m = 278$ MHz, τ_{output} was observed to equal 140 ps. For FM mode-locking, τ is given by Equation 1 multiplied by $\sqrt{2}$. This gives $\tau = 44$ ps, which yields a diode rise time of 80 ps.

The remaining three tubes were tested for response to the second harmonic wavelength. Figure 7a shows the photodiode response to a 1.06-μm mode-locked pulse and Figure 7b shows the same photodiode response to a 0.53-μm pulse, the result of frequency doubling the pulse shown on Figure 7a. The time scale for both photographs is 200 ps/cm. The 1.06-μm pulse is measured to be 187 ps and the 0.53-μm pulse is measured to be 130 ps. This agrees within experimental error with the expected ratio between Equations 3 and 5. Therefore when testing 0.53-μm detectors, the 1.06-μm pulsewidth is measured and the value is divided by $\sqrt{2}$ to get the 0.53-μm signal rise and fall times.

Figure 8 shows the response of the second detector to focused 0.53-μm mode-locked pulses. The time scale on Figure 8a is 1 ns/cm and on Figure 8b is 500 ps/cm. Results show that τ_r = 670 ps and τ_f = 750 ps for this detector. Thus the tube can be used for detecting 200-ps 0.53-μm pulses up to a repetition rate of 590 MHz. (The slight waviness in the detector traces of Figures 8, 9, and 10 is caused by rf interference from the mode-locker.)

The speed of response of the second detector was measured as a function of voltage applied to the tube. Figure 8 was obtained with the tube operating at the optimum voltage, 2900 V. In addition, response was measured for unfocused and unattenuated light. Figure 9a shows the response of the second detector to a focused but unattenuated input; here τ_r = 710 ps and τ_f = 920 ps. Figure 9b shows the response to an unfocused input, attenuated by an 0.3 neutral density filter. Here τ_r = 670 ps and τ_f = 830 ps. The time scale in Figure 9 is 500 ps/cm.

Figure 10 shows the response of the third detector to 0.53-μm mode-locked pulses. The time scale of Figure 10a is 1 ns/cm and Figure 10b is 500 ps/cm. These photographs show that for this detector τ_r = 510 ps and τ_f = 660 ps. This response limits the tube to mode-locked frequencies of less than 710 MHz for 200-ps pulses. The input beam was focused to give the best speed of response. The three focusing electrode potentiometers shown in Figure 4 were adjusted to give optimum response.

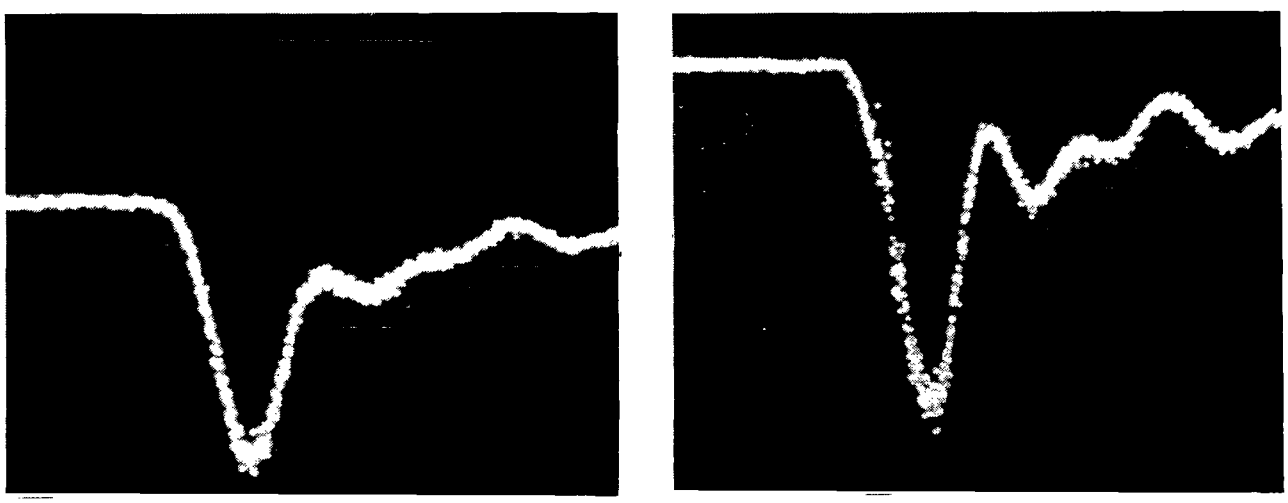

(a) (b)

Figure 7—Photodiode response. Time scale: 200 ps/cm; vertical scale: 5 mV/cm. (a) Response of the photodiode to 1.06-μm pulses. (b) Response of the same photodiode to 0.53-μm pulses generated by frequency doubling the 1.06-μm pulses of Figure 7a.

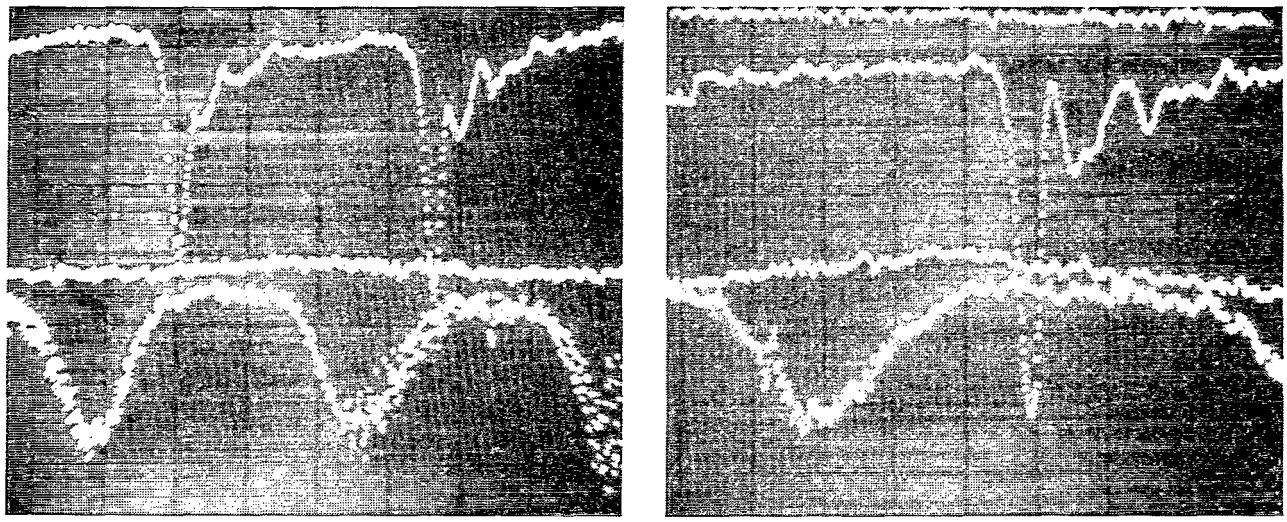

(a) (b)

Figure 8—The upper trace on both parts of the figure shows the photodiode response to 1.06-μm pulses (vertical scale: 5 mV/cm). The lower trace on both parts of the figure shows the response of the second detector to 0.53-μm pulses focused on the photocathode. The 0.53-μm pulses were obtained by frequency doubling the 1.06-μm pulses. (a) Time scale: 1 ns/cm. The 0.53-μm pulses were attenuated by a 0.3 neutral density filter. Vertical scale for the trace of the second detector is 5 mV/cm. (b) Time scale: 500 ps/cm. The 0.53-μm pulses were attenuated by a 0.5 neutral density filter. The vertical scale for the second detector is 2 mV/cm.

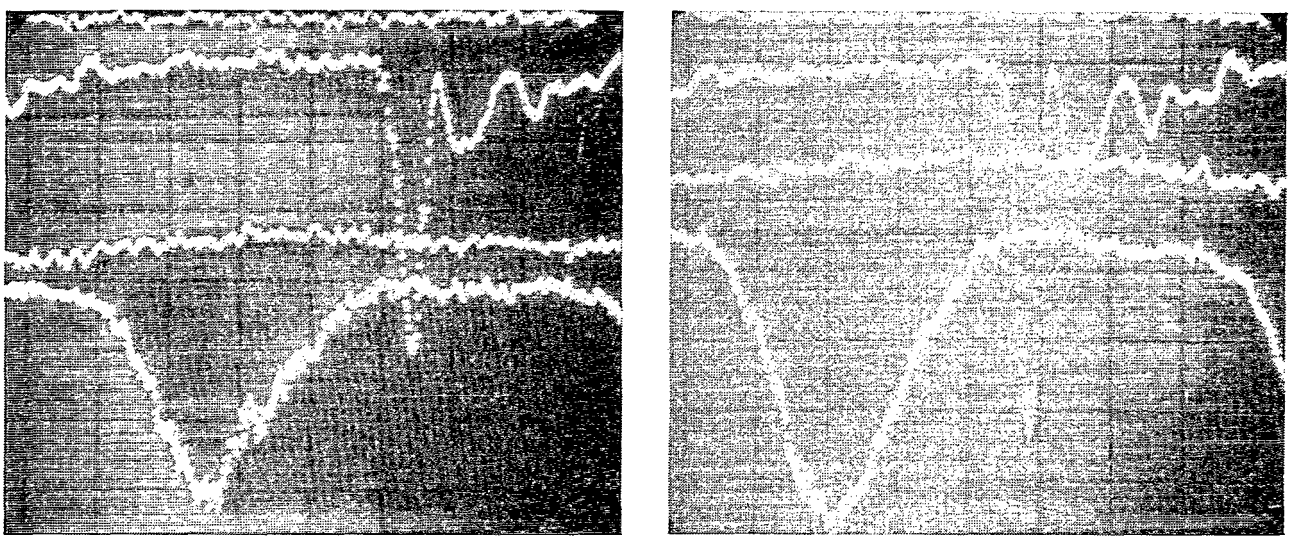

(a) (b)

Figure 9—The upper trace on both parts of the figure shows the photodiode response to 1.06-μm pulses (vertical scale: 5 mV/cm). Time scale: 500 ps/cm. (a) The lower trace is the response of the second detector to unattenuated, focused 0.53-μm pulses obtained by frequency doubling the 1.06-μm pulses (vertical scale: 2 mV/cm). (b) The lower trace is the response of the second detector to unfocused 0.53-μm pulses attenuated by a 0.3 neutral density filter (vertical scale: 2 mV/cm).

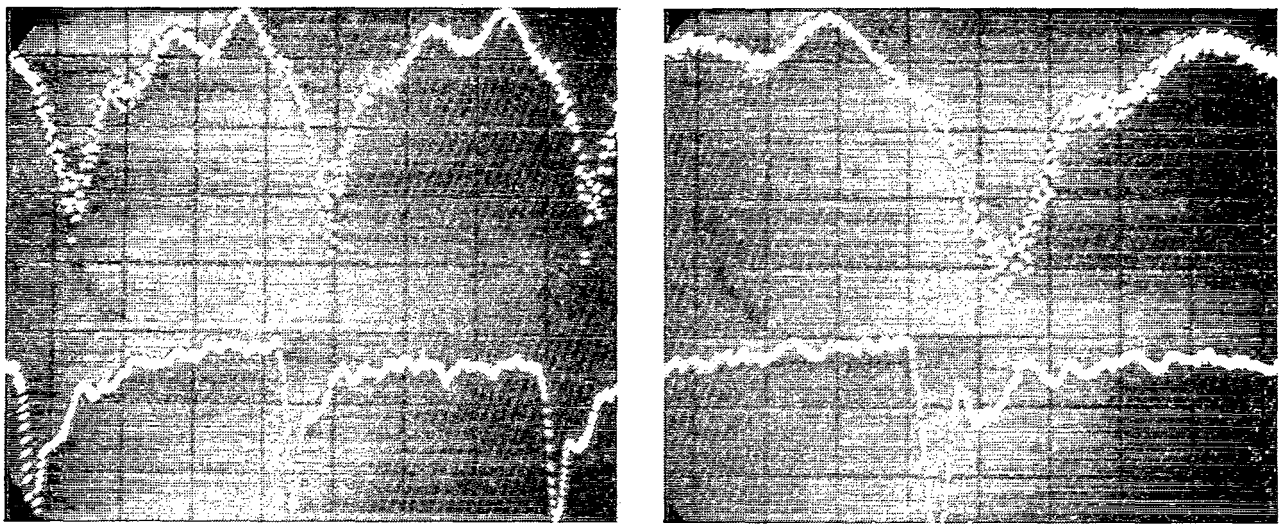

(a) (b)

Figure 10—The lower trace on both parts of the figure shows the photodiode response to 1.06-μm pulses (vertical scale: 2 mV/cm). The upper trace on each part of the figure shows the response of the third detector to 0.53-μm pulses generated by frequency doubling the 1.06-μm pulses (vertical scale: 20 mV/cm). (a) Time scale: 1 ns/cm. (b) Time scale: 500 ps/cm.

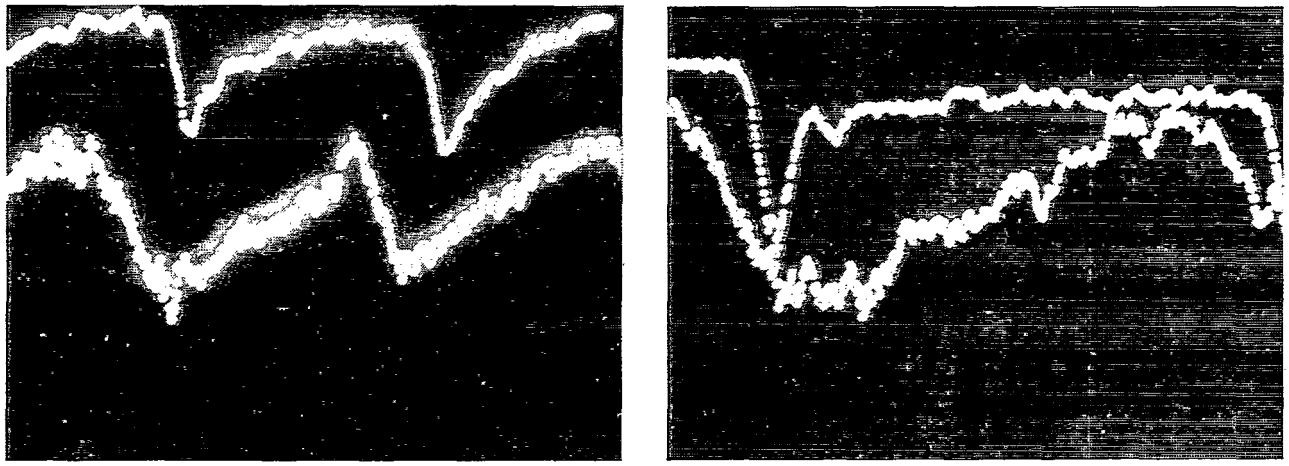

(a) (b)

Figure 11—The upper trace on both parts of the figure shows the photodiode response to 1.06-μm pulses (vertical scale: 1 mV/cm). The lower trace on each part of the figure shows the response of the fourth detector to 0.53-μm pulses generated by frequency doubling the 1.06-μm pulses (vertical scale: 1 mV/cm). (a) Time scale: 1 ns/cm. (b) Time scale: 500 ps/cm.

The response of the fourth detector is shown in Figure 11. Here τ_r = 670 ps and τ_f = 1.75 ns. Response is limited to frequencies below 275 MHz, mainly because of the relatively poor fall time.

CONCLUSION

The technique described in the previous sections for measuring speed of response of high-speed optical detectors is relatively easy to apply and gives consistent results. On the basis of tests of the four detectors, it is found that the first three detectors can be used in a 500-MHz PCM optical communication system when the detector output is integrated over each pulse period without introducing intersymbol interference. The fourth detector can be used as a detector in the same type of system operating at about 270 MHz without introducing intersymbol interference.

ACKNOWLEDGMENT

The authors thank Robert Anderson for expert technical help in the fabrication of components.

Goddard Space Flight Center
National Aeronautics and Space Administration
Greenbelt, Maryland, February 24, 1972
115-22-08-01-51

REFERENCES

1. Geusic, J. E.; Marcos, H. M.; and Van Uitert, L. G.: "Laser Oscillations in Nd-Doped Yttrium Aluminum, Yttrium Gallium, and Gadolinium Garnets." *Appl. Phys. Lett.* **4**: 182, May 15, 1964.

2. Di Domenico, M., Jr.; Geusic, J. E.; Marcos, H. M.; and Smith, R. G.: "Generation of Ultrashort Optical Pulses by Mode Locking the YAlG:Nd Laser." *Appl. Phys. Lett.* **8**: 180-183, April 1, 1966.

3. Osterink, L. M.; and Foster, J. D.: "A Mode-Locked Nd:YAG Laser." *J. Appl. Phys.* **39**: 4163-4165, Aug. 1968.

4. Kuizenga, D. J.; and Siegman, A. E.: "FM and AM Mode-Locking of the Homogeneous Laser—Pt. I: Theory." *IEEE J. Quantum Electron.* **6**: 694-708, Nov. 1970.

5. Hoth, D. F.: "Digital Communication." *Bell Lab. Rec.* **45**: 39-44, Feb. 1967.

6. Kelley, R. A.: "An Experimental High-Speed Digital Transmission System." *Bell Lab. Rec.* **45**: 45-48, Feb. 1967.

7. Kinsel, T. S.: "Light Wave of the Future: Optical PCM." *Electronics* **41**: 123-128, Sept. 16, 1968.

8. Blombergen, N.: "Some Theoretical Problems in Quantum Electronics." *Proc. Opt. Masers,* Polytechnic Press, Polytechnic Inst. of Brooklyn, pp. 13-23, 1963.

9. Valley, G. E., Jr.; and Wallman, H.: *Vacuum Tube Amplifiers,* McGraw-Hill Book Co., Inc., pp. 77-78, 1948.

NASA-Langley, 1972 —— 16

"The aeronautical and space activities of the United States shall be conducted so as to contribute . . . to the expansion of human knowledge of phenomena in the atmosphere and space. The Administration shall provide for the widest practicable and appropriate dissemination of information concerning its activities and the results thereof."

—NATIONAL AERONAUTICS AND SPACE ACT OF 1958

NASA SCIENTIFIC AND TECHNICAL PUBLICATIONS

TECHNICAL REPORTS: Scientific and technical information considered important, complete, and a lasting contribution to existing knowledge.

TECHNICAL NOTES: Information less broad in scope but nevertheless of importance as a contribution to existing knowledge.

TECHNICAL MEMORANDUMS: Information receiving limited distribution because of preliminary data, security classification, or other reasons.

CONTRACTOR REPORTS: Scientific and technical information generated under a NASA contract or grant and considered an important contribution to existing knowledge.

TECHNICAL TRANSLATIONS: Information published in a foreign language considered to merit NASA distribution in English.

SPECIAL PUBLICATIONS: Information derived from or of value to NASA activities. Publications include conference proceedings, monographs, data compilations, handbooks, sourcebooks, and special bibliographies.

TECHNOLOGY UTILIZATION PUBLICATIONS: Information on technology used by NASA that may be of particular interest in commercial and other non-aerospace applications. Publications include Tech Briefs, Technology Utilization Reports and Technology Surveys.

Details on the availability of these publications may be obtained from:

SCIENTIFIC AND TECHNICAL INFORMATION OFFICE

NATIONAL AERONAUTICS AND SPACE ADMINISTRATION

Washington, D.C. 20546